JOURNAL OF MATERIALS SCIENCE 30 (1995) 1894–1901

Compressive strength of coated rigid-rod polymer fibres

U. SANTHOSH*
AdTech Systems Research Inc., 1342 North Fairfield Road, Dayton, OH 45432, USA

K. E. NEWMAN
Central Research and Development, E.I. DuPont De Nemours & Co. Inc., P.O. Box 80304, Wilmington, DE 19880, USA

C. Y-C. LEE
AFOSR/NC, Air Force Office of Scientific Research, Bolling Air Force Base, DC 20332, USA

One limitation to the use of high-strength/high-modulus rigid-rod polymer fibres like poly-(*p*-phenylene benzobisthiazole) (PBZT) and poly-(*p*-phenylene benzobisoxazole) (PBZO) in composite structures is their low compressive strength. Various theories have been developed to predict compressive strength of rigid-rod fibres. In this study the critical buckling stress for rigid-rod fibres with stiff external coatings has been theoretically modelled assuming that the failure mode in compression is the microbuckling of the fibrils in shear. Our model predicts that significant improvement in fibre compressive strength will occur only when relatively thick coatings, with thickness to diameter (t/D) ratios in excess of > 0.05, are used. Experimentally measured compressive strength of aluminium coated PBZT fibres shows values in good agreement to the theory at t/D ratios of 0.006 and below. Factors related to the selection of suitable coating materials and problems associated with establishing coating performance are identified.

Nomenclature

P	axial compressive load
P_f	axial compressive load on the fibre
P_c	axial compressive load on the coating
P_{cr}^i	critical buckling load in the ith case
σ_{cr}	critical buckling stress
σ_{co}	compressive strength of the uncoated fibre
σ_c	compressive strength of the coated fibre
$v(x)$	lateral deflection of a buckled fibril or coating
V_m	amplitude of the lateral deflection in the mth mode
m	number of half-sine waves in the deflection mode
x	coordinate distance along axial direction
y	coordinate distance along radial direction
θ	coordinate distance along circumferential direction
l	length of the buckling unit
N	number of fibrils in the fibre
D	fibre diameter
d	fibril diameter
t	coating thickness
I_f	moment of inertia of the fibril
A_f	cross-sectional area of the fibril
E_f	tensile modulus of the fibre
E_c	tensile modulus of the coating material
E	tensile modulus of the coated fibre
G	torsional shear modulus of the fibre
ν_c	Poisson's ratio of the coating material
ρ_f	density of the fibre
ρ_c	density of the coating material
ρ	density of the coated fibre
ΔU_f	strain-energy change in the fibre
ΔU_c	strain-energy change in the coating
ΔT_f	external work done on the fibre
ΔT_c	external work done on the coating
ξ	d/D
η	t/D

1. Introduction

Rigid-rod polymer fibres of the heterocyclic aromatic type, like poly-(*p*-phenylene benzobisthiazole) (PBZT) and poly-(*p*-phenylene benzobisoxazole) (PBZO), are known to have high specific stiffness and strength [1]. They also exhibit thermal stability up to 700 °C, and excellent chemical and environmental resistance. Unfortunately, their potential use in high-performance composite applications is severely limited by poor compressive strength [1]. This class of fibres have a fibrillar morphology with the fibrils made up of highly oriented polymer chains. It is currently thought that the oriented fibrils/chains which give the polymer its high tensile properties is also responsible for its low transverse properties and low compressive strength [2, 3].

Much of the research towards improving the compressive strength of these fibres has been focused

* *Present address*: Research Applications Inc., 7026 Corporate Way, Suite 211, Centerville, OH, 45459, USA.

0022–2461

on cross-linking the polymer chains during heat treatment [4], irradiation [5] or via hydrogen bonding [6]. Implicit in the above studies is the assumption that the source of the low compressive strength is poor intermolecular interaction. Therefore, any improvement in the degree of lateral interaction between the PBZX molecules would improve the macroscopic fibre compressive strength. No conclusive evidence exists that defines which, if any, of these methods have had an augmenting effect on the compressive strength. Few experimental studies have identified the operative mechanism of failure for PBZX fibres under compressive loading. Martin and Thomas [3] reported the model of failure in PBZX fibres after compressive loading to be macrofibrillar buckling. Kovar *et al.* attempted to infiltrate freshly spun fibres with a sol–gel glass in an effort to provide lateral stability between the microfibrils with questionable success [7].

Theoretical microbuckling models have also been used to explain the compressive failure mechanism in these fibrillar, anisotropic fibres in terms of the collective buckling of fibrils and /or chains [2]. It has been pointed out in an earlier paper [8] that the observed low compressive strength is most likely determined by the lowest of all the different buckling modes at the various microstructure levels in the fibre. In fact, good correlation has been reported between the compressive strength and the shear modulus of several anisotropic polymer fibres including PBZT [9]. If the above argument holds, then any improvement in the lateral interaction between the fibrils, shear or otherwise, should improve the compressive strength.

It has been demonstrated by Newman *et al.* [10] that PBZT can be immersed into molten aluminium alloy to temperatures as high as 700 °C for times greater than 1 min, and maintain 75% of its as-received tensile strength; immersions at lower temperatures permitted correspondingly longer dwell times for the same drop in observed strength. Also they found that the application of physically vapour-deposited aluminium overlayers under high-vacuum deposition conditions, followed by thermal annealing at temperatures of 600 °C, caused a drop in strength which could be recovered if the aluminium overlayer was removed prior to testing. No data were presented on the effect of aluminium contact on the compressive strength of this fibre.

Therefore, in the present work it was decided to study the effect of coating PBZT fibres with aluminium. The aim was to study the effect of the metal on the fibre compressive strength either by the possible infiltration of the metal into the fibre interior or by the coating acting as a rigid outer support and inhibiting the buckling of the fibre.

2. Buckling of coated fibrillar fibres

In the following analysis we shall assume that the compressive failure of the rigid-rod fibre is determined by the microscopic buckling of the fibrils in the shear mode. This assumption is supported by the SEM observations of shear zones around kink bands and the good linear correlation between the torsional shear modulus and the compressive strength of these fibres. For this mode of buckling the theoretical compressive strength of the fibrillar fibre can be approximated by its torsional shear modulus, G [2]. Thus, if a metal such as aluminium is infiltrated between the fibrils, the improved adhesion between the fibrils will result in an increase in the value of G and hence the compressive strength. Here it is also assumed that the primary unit responsible for failure is not influenced by the support of the shell of material around the fibre.

On the other hand, the incorporation of a coating around the fibre can also affect its compressive strength even if the material does not infiltrate into the fibrils. One way would be for the rigid coating to inhibit the local buckling or kinking of enclosed polymer fibre by restraining the folding of the fibrils (Fig. 1b). In this situation the fibre in contact with the isotropic coating will cause hoop strains in the latter which will increase the total strain energy of the system. By assuming that the axial load acts on the coating only through the deformation of the fibre, we can use the energy method [11] to determine the critical load for buckling of the system.

Consider a fibre of diameter, D, coated through a thickness, t. We assume that an axial compressive force, P, causes the fibre and the fibrils to deform in

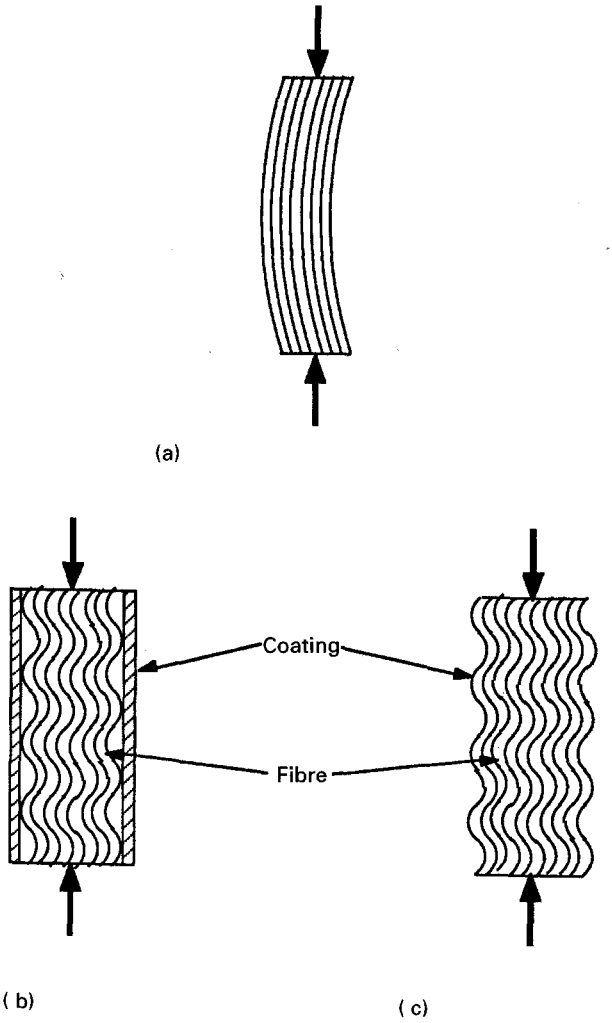

Figure 1 (a) Shear-mode failure in an uncoated fibre. (b) Fibre buckling constrained by rigid coating (poor adhesion between coating and fibre). (c) Combined buckling of coating and fibre (good adhesion between coating and fibre).

a sinusoidal manner so that the lateral deflection is of the form

$$v(x) = V_m \sin(m\pi x/l) \quad (1)$$

Here the mode number, m, represents the number of peaks (minima or maxima) in the lateral deformation shape of the fibre. If d is the diameter of the single fibrils comprising the fibre and if l is the length of the buckling unit, then the increase in the strain energy of the fibre caused by the load can be derived as [2, 11]

$$\Delta U_f = \left(\frac{\pi^4 E_f I_f}{4l^3}\right) m^4 V_m^2 + \left(\frac{\pi^2 G A_f}{4l}\right) m^2 V_m^2 \quad (2)$$

In the above expression E_f and G denote the tensile and the torsional shear moduli of the fibre, while $A_f = \pi d^2/4$ and $I_f = \pi d^4/64$ are the average area and moment of inertia of a single fibril respectively. Similarly the work done by the axial load on the fibre is given by

$$\Delta T_f = \left(\frac{P\pi^2}{4l}\right) m^2 V_m^2 \quad (3)$$

If the coating is made to deform by the fibre in contact with it, we can assume that the circumferential deformation of the coating is also be given by Equation 1. The hoop strain energy of the coating with stiffness, E_c, will then be

$$\begin{aligned}\Delta U_c &= \int_0^l \int_0^{2\pi} \int_{D/2}^{D/2+t} \frac{E_c}{2} \frac{V_m^2 \sin^2(m\pi x/l)}{(D/2+t)^2} \mathrm{d}y \\ &\quad \times \frac{(D+t)}{2} \mathrm{d}\theta \, \mathrm{d}x \\ &= \frac{E_c}{2} \frac{\pi(D+t)t}{(D/2+t)^2} \frac{l}{2} V_m^2 \end{aligned} \quad (4)$$

Applying the energy method, the total load required to buckle this system in the mth mode can be determined from the condition

$$N\Delta U_f + \Delta U_c = \Delta T_f \quad (5)$$

Here $N \approx D^2/d^2$ is the number of fibrils in the fibre. Substituting Equations 2, 3 and 4 in Equation 5 and simplifying, we have the following expression for the total load to buckle the fibre in the mth mode.

$$\begin{aligned} P_{cr}^1 &= \left(\frac{\pi^3 E_f D^2 d^2}{64 l^2}\right) m^2 + \frac{\pi G D^2}{4} \\ &\quad + \left[\frac{4E_c(D+t)tl^2}{\pi(D+2t)^2}\right] \frac{1}{m^2} \end{aligned} \quad (6)$$

Minimizing the above equation with respect to the mode number, the buckling mode corresponding to the lowest critical buckling load and the corresponding critical bucking stress is determined to be

$$m^2 = \frac{16l^2}{\pi^2(D+2t)Dd}\left[\frac{E_c}{E_f}(D+t)t\right]^{1/2} \quad (7)$$

$$\begin{aligned}\sigma_{cr}^1 &= \frac{4P_{cr}^h}{\pi(D+2t)^2} \\ &= G\frac{1}{(1+2\eta)^2} + \frac{2\xi}{(1+2\eta)^3}[E_f E_c \eta(1+\eta)]^{1/2} \end{aligned} \quad (8)$$

respectively, where $\xi = d/D$ and $\eta = t/D$.

In the above analysis, it is assumed that the compressive load does not act on the coating and that there is no fraction between the coating and the fibre. However, a more realistic model is one in which the shell of material shares some of the axial load and the strong adhesion between the fibre and the coating results in combined local buckling as shown in Fig. 1c. In such a model, the coating can be treated as a thin shell subjected to an axial compressive load, P_c. It has been shown elsewhere [12] that for long isotropic cylinders with a sufficiently rigid, isotropic core, the buckling stresses in the axisymmetric mode is lower than that of the other, more general modes. Because the modulus of the core (PBZO or PBZT) is comparable to that of the coating material, we shall consider the axisymmetric deformation of the outer coating and calculate buckling stress.

By assuming the deformation of the thin coating of the form given in Equation 1, the procedure outlined by Timoshenko and Gere [11] can be used to determine the change in the strain energy, ΔU_c, due to an externally applied compressive load and also the work done by the load, ΔT_c. The respective expressions are

$$\begin{aligned}\Delta U_c &= -2\pi E_c \nu_c t \left(\frac{-P_c}{\pi(D+t)} \frac{1}{E_c t}\right) \int_0^l V_m \sin(m\pi x/l)\mathrm{d}x \\ &\quad + \frac{\pi E_c V_m^2 tl}{(D+t)} + V_m^2 \left(\frac{m^4\pi^4}{2l^4}\right)\left[\frac{\pi(D+t)l}{2}\right] \\ &\quad \times \left[\frac{E_c t^3}{12(1-\nu_c^2)}\right] \\ &= \frac{2P_c \nu_c V_m l}{m\pi(D+t)}[1-\cos(m\pi)] + \frac{\pi E_c V_m^2 tl}{(D+t)} \\ &\quad + \left[\frac{m^4\pi^5 V_m^2(D+t)}{4l^3}\right]\left[\frac{E_c t^3}{12(1-\nu_c^2)}\right] \end{aligned} \quad (9)$$

$$\begin{aligned}\Delta T_c &= 2\pi\left[\frac{P_c}{\pi(D+t)}\right]\left\{\nu_c \int_0^l V_m \sin(m\pi x/l)\mathrm{d}x \right. \\ &\quad \left. + \left(\frac{m^2\pi^2}{l^2}\right)\left[\frac{V_m^2(D+t)}{8}\right]\right\} \\ &= \frac{2P_c}{(D+t)}\left\{\frac{\nu_c V_m l}{m\pi}[1-\cos(m\pi)] \right. \\ &\quad \left. + \left(\frac{m^2\pi^2}{l}\right)\left[\frac{V_m^2(D+t)}{8}\right]\right\} \end{aligned} \quad (10)$$

Here ν_c denotes the Poisson's ratio coating material. In the case of the fibre, the change in the strain energy, ΔU_f, due to an externally applied compressive load and the work done by the load, ΔT_f, is obtained from Equations 2 and 3, respectively, by replacing the total load, P, by the component, P_f, which acts only on the fibre. Applying the energy method, the limiting condition for instability becomes

$$N\Delta U_f + \Delta U_c = \Delta T_f + \Delta T_c \quad (11)$$

Substituting for the changes in the strain energy and the external work done in the above equation and the expressions for the total load required to buckle such

a system ($P_{cr} = P_f + P_c$) the minimum critical buckling stress for this case are

$$P_{cr}^2 = \left(\frac{\pi^3 E_f D^2 d^2}{64 l^2}\right) m^2 + \frac{\pi G D^2}{4} + \left[\frac{4 E_c t l^2}{\pi(D+t)}\right]\frac{1}{m^2} + \left[\frac{\pi^3 E_c (D+t) t^3}{12(1-\nu_c^2) l^2}\right] m^2 \quad (12)$$

and

$$\sigma_{cr}^2 = G\frac{1}{(1+2\eta)^2} + \frac{8\xi}{(1+2\eta)^2} \times \left\{E_c \frac{\eta}{(1+\eta)}\left[\frac{E_f}{16} + \frac{E_c}{3(1-\nu_c^2)}\frac{\eta^3(1+\eta)}{\xi^2}\right]\right\}^{1/2} \quad (13)$$

respectively. This stress corresponds to the buckling mode given by

$$m^2 = \frac{2l^2}{\pi^2}\left[E_c \frac{t}{(D+t)}\right]^{1/2} \times \left[\frac{E_f D^2 d^2}{64} + (D+t)\frac{E_c t^3}{12(1-\nu_c^2)}\right]^{-1/2} \quad (14)$$

Because the torsional shear modulus of the fibre, G is very small compared to the tensile modulus of the isotropic coating, we shall consider a third case, wherein only the strain energy in the coating is considered in determining the minimum stress for instability of the coated fibre. The minimum critical buckling stress for a thin cylindrical shell has been derived by Timoshenko and Gere [11] as

$$P_{cr}^3 = 2\pi t^2 \frac{E_c}{[3(1-\nu_c^2)]^{1/2}} \quad (15)$$

The corresponding stress causing instability in the coated fibre then becomes

$$\sigma_{cr}^3 = \frac{8\eta^2}{(1+2\eta^2)}\frac{E_c}{[3(1-\nu_c^2)]^{1/2}} \quad (16)$$

Using the values for the moduli of the fibre and coating materials given in Tables I and II, respectively, the increase in the compressive strengths (σ_{cr}/G) of the aluminium-coated PBZT fibre and ceramic-coated PBZO fibre, as predicted by Equations 8, 13 and 16, are plotted in Figs 2 and 3, respectively. For PBZT the fibril dimensions were estimated from scanning electron micrographs of peeled fibres; the values for PBZO fibre were taken from [13]. It can be seen that for relatively small coating thickness, there is no significant effect on the compressive strength; beyond $t/D = 0.01$ there is a sharp increase in the compressive strength. The increase is significant only when the combined buckling of the fibre and coating is taken into account (Equation 13). On the other hand, when the coating is considered to have only a hoop-restraining effect on the fibre, the apparent increase in the compressive strength is small. It can also be seen that as the coating thickness increases, the compressive strength of the fibre–coating composite (Equation 13) approaches that of just the cylindrical shell of coating material (Equation 16). This is due to the relatively low value of the torsional shear modulus of the rigid-rod polymer fibres as compared to the tensile modulus of the coating materials which, in turn, implies that for sufficiently thick coatings the buckling strength of the coated fibre is governed by that of the rigid shell.

TABLE I Properties of rigid-rod polymer fibres

Property	PBZT	PBZO
E_f (GPa)	300	310 [13]
G (GPa)	1.2 [9]	1.2[a]
ρ_f (kg m^{-3})	1580 [1]	1580 [1]
D (μm)	16	24 [13]
d (μm)	0.2	0.2 [13]

[a] Assumed to be similar to that for PBZT.

TABLE II Properties of coating materials

Property	Aluminium	Ceramic[a]
E_c (GPa)	69	275
ν_c	0.3	0.2
ρ_c (kg m^{-3})	2700	3100

[a] Representative properties of ceramic material.

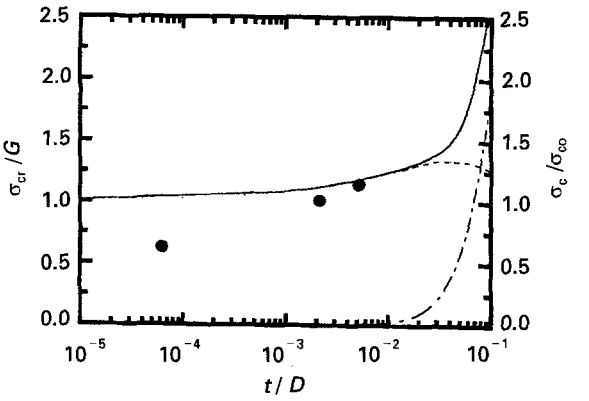

Figure 2 Compressive strength of aluminium-coated PBZT fibre. (– – –) Equation 8, (——) Equation 13, (— — —) Equation 16, (●) experimental data.

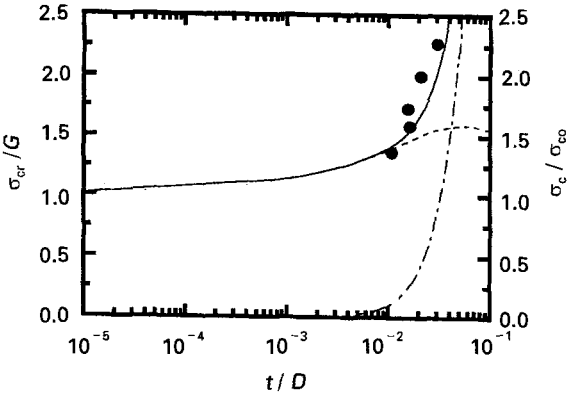

Figure 3 Compressive strength of ceramic-coated PBZO fibre. (– – –) Equation 8, (——) Equation 13, (— — —) Equation 16, (●) experimental data [13].

3. Experimental procedure

The PBZT fibre used in all experiments was spun at the DuPont Experimental Station under an Air Force contract by the dry-jet wet spun process, dried, and heat treated at approximately 575 °C for 10 s under a nitrogen shield gas. Nominal fibre diameter was determined from measurement of 50 filaments as 15.9 ± 0.9 μm.

Samples of the PBZT fibre were coated with high-purity aluminium (99.999%) by vacuum evaporation at ambient temperature. Prior to coating, the fibre samples were mounted on to a "rotisserie" used to rotate the fibres during deposition, thus maintaining a uniform layer of metal on to the fibre. A schematic drawing of the fibre rotisserie unit used is shown in Fig. 4. Coating occurred in a large bell jar maintained at 10^{-7}–10^{-8} torr (1 torr = 133.322 Pa). The pure aluminium wire was held in a tungsten filament basket which was resistively heated until the aluminium vaporized, at which time a shutter was opened and aluminium vapour entered the chamber. Coating thickness was monitored by an oscillating quartz crystal. Transmission electron microscopy of coated fibre cross-sections confirms the uniformity in coating thickness.

After coating, the PBZT fibres were removed from the rotisserie and mounted on paper tabs of 25. 4 mm (1 in) gauge section using Cole-Palmer 5-Minute Epoxy©. Once the epoxy was cured, but prior to testing, the fibre diameter was measured in three places using a filar eyepiece on an optical microscope and averaged. The compression testing of the fibres was next done by the fibre recoil test method [14]. The test is based on the principle that the application of a controlled tensile pre-load to the fibre, followed by rapid breakage of the fibre (induced by cutting), results in a tensile stress wave travelling from the break, up the fibre length, until the wave reaches the rigid fibre end. At this point the tensile wave changes to an equal but opposite magnitude compressive wave. If the compressive stress generated is higher than the compressive strength of the fibre, the fibre fails. In high-performance polymeric fibres, the fibre failure is manifested by kink band formation which is observed optically. The test procedure is repeated using new specimens until a lower tensile stress is found below which no kink bands are observed when the specimen is cut. The compressive strength of the fibre is then taken to be the mean of the two limiting values of the tensile stress. The tests reported in this work were performed on a bench-top Instron tensile machine using a 50 g capacity load cell and spring-loaded grips. An electric arc was used to cut the fibre during the recoil test. All reported compressive strength values are the result of a minimum of twenty tests.

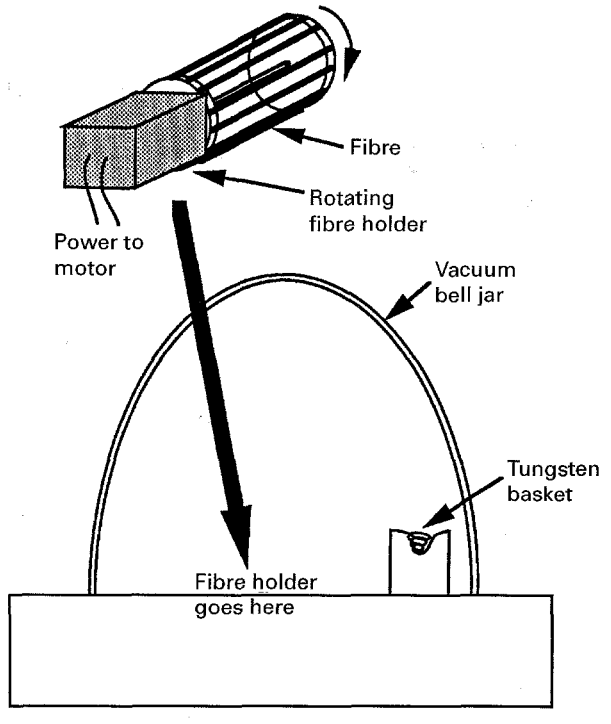

Figure 4 Vapour deposition apparatus for aluminium coating of PBZT fibre.

4. Results and discussion

Results from the recoil tests on the as-received and the coated PBZT fibres are shown in Table III. As can be seen, the compressive strength of PBZT fibre does not seem to increase significantly as the coating thickness approaches 833 nm. The drop in compressive strength corresponding to the 10 nm coating thickness may be due to handling problems encountered during the preparation of the fibres for mental deposition. Subsequent metal depositions were done in a more careful fashion to prevent possible damage of the fibre and did not show the same drop in strength. The usual method to detect compressive failure in polymer fibres is to observe the fibre optically via transmitted light for kink bands. It was not possible to see through the fibres possessing 34.4 and 83.3 nm thick aluminium coatings and detect the same level of kink bands as could be resolved on the transparent fibres, i.e. the as-received or 1 nm aluminum-coated fibres, therefore the compressive strengths reported for these cases must be considered as upper limits. Thus in order to establish if the fibre is indeed kinked in the coated fibre systems other techniques aside from optical inspection, as is currently the practice, may be required.

Field-emission microscopy shows the metal–polymer interface to be poor as evinced by the large amount of cracking in the coating and the appearance that the coating simply lies on the fibre surface (Fig. 5). There is also no evidence of the metal having infiltrated into the fibre. Adhesion measurements made of aluminium-coated PBZT films indicate that no

TABLE III Compressive strength of aluminium-coated PBZT fibres

Coating thickness (nm)	Compressive strength (MPa)
0	231 ± 10
1.0	145 ± 20
34.4	234 ± 10
83.3	265 ± 10

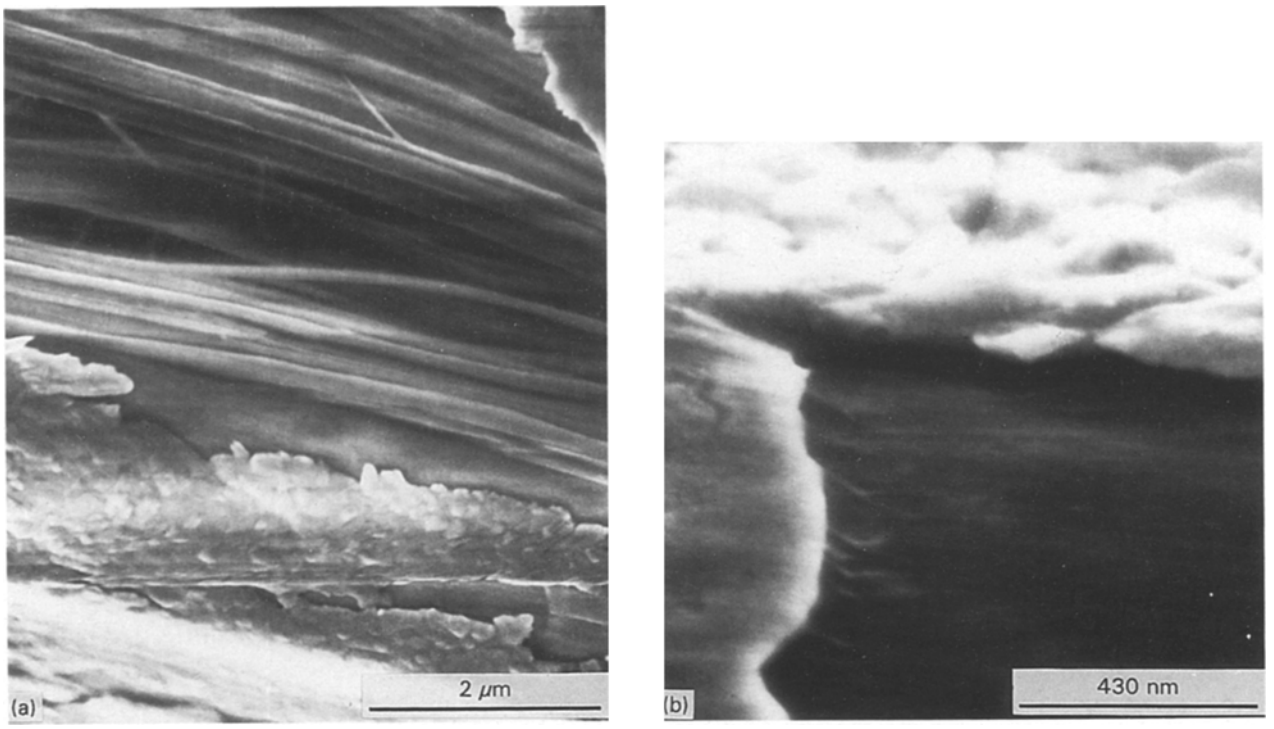

Figure 5 (a, b) High-resolution scanning electron micrographs of an aluminium-coated PBZT fibre.

appreciable adhesion exists between the metal and the polymer as observed by the entire aluminium coating coming off when peeled with Scotch tape [15]. Fig. 6 shows the aluminium coating to be a microcrystalline aggregate with an average crystallite size of 144 ± 0.3 nm. The rough surface could act as a stress concentrator, either in tension or compression. Therefore, it would be desirable to have a microscopically smooth, uniform coating to eliminate this possible influence.

Fig. 2 compares the theoretically predicted increase in the shear mode buckling stress with the experimentally determined increase in the value of the recoil compressive strength, σ_c, for aluminium-coated PBZT fibres. The subscript 'o' used in the figure denotes the uncoated fibre. It can be seen that the experimental and theoretical values agree reasonably well and that in the range of the coating thickness used in the experiment the compressive strength is not expected to increase significantly. As mentioned earlier, because the aluminium coating does not adhere well to the PBZT fibre surface and as the coating is not very uniform, it is more likely for the actual compressive behaviour to be described by Equation 8.

The validity of the theoretical model is further established by comparing its results for ceramic-coated PBZO fibres with experimentally determined values of the compressive strength from [13] (Fig. 3). Again, the correlation is quite good, but the theoretical model that best describes the compressive strength of the coated fibre in this case seems to be that which considers the combined buckling of the polymer fibre and the ceramic coating (Equation 13). This may be attributed to the ceramic coating having a smooth and homogeneous structure and adhering well to the PBZO fibre, as stated elsewhere [13].

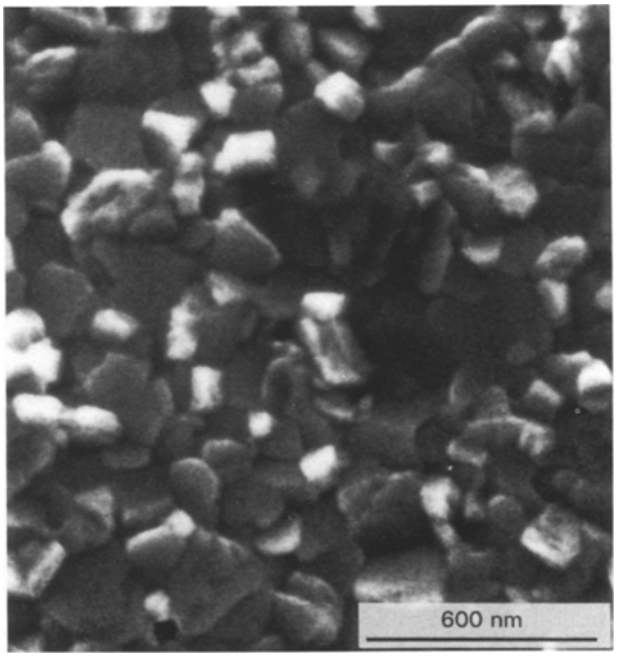

Figure 6 High-resolution scanning electron micrograph of the aluminium coating applied to a fibre surface.

Fig. 7 shows the theoretically predicted increase in compressive strength of the rigid-rod fibres due to a rigid coating. It is assumed that there is perfect adhesion between the coating and the fibre and so Equation 13 is used. The variation in the compressive strength has been plotted up to $t/D = 0.1$, which is the limit of the thin shell theory used in the theoretical analysis. Because there is not much difference between the tensile moduli of PBZO and PBZT, the two curves can be used interchangeably. It can be noted that aluminium is a poor choice as the coating material

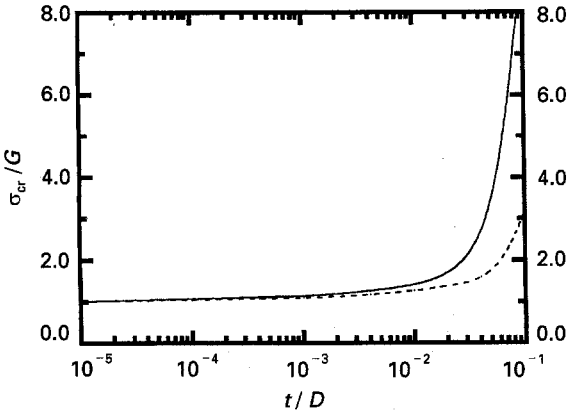

Figure 7 Improved compressive strength of rigid-rod polymer fibres. (– – – –) Aluminium coated PBZT, (——) ceramic-coated PBZO.

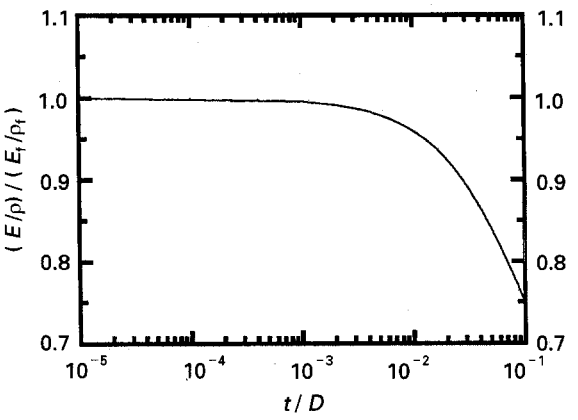

Figure 8 Specific tensile modulus of ceramic coated PBZO fibre.

because the compressive strength cannot be increased by more than a factor of three, as compared to the uncoated fibre, even if perfect bonding can be ensured between it and the polymer fibre. On the other hand, if the high-modulus ceramic is used as the coating material, a coating thickness of about 0.08 D is sufficient in order to achieve a compressive strength of about 1.4 GPa ($\sigma_{cr}/G = \sigma_c/\sigma_{co} = 6$–$7$).

In addition to the effect on the compressive strength, placing a coating on the polymer fibre will also change its modulus and density. Rule-of-mixture approximations can be used to predict the tensile modulus and the density of the fibre-coating composite. Because ceramic is a better choice as a coating material than aluminium, as shown above, we shall consider the modulus and density of ceramic-coated PBZO fibres. For a coating thickness of $0.8D$, rule of mixtures yields $E \equiv \bar{E}/E_f = 0.97$. For the same coating thickness, the density of the coated PBZO can be determined to be given by $\rho \equiv \bar{\rho}/\rho_f = 1.25$. Here the bar quantities represent the properties of the composite. In high-performance applications the tensile modulus per unit weight is usually used to evaluate the efficiency of a structural member. Fig. 8 plots the variation of the specific tensile modulus of the coated fibre, E/ρ, with the coating thickness. For $t/D = 0.8$, this factor for the coated fibre can be seen to have decreased by about 22% when compared to that of the uncoated PBZO fibre. Thus the trade-off in achieving a higher value of compressive strength by coating the rigid-rod polymer fibre is the reduction in its stiffness per unit weight.

5. Conclusion

Buckling equations have been presented to describe the compressive failure in coated fibres possessing a fibrillar microstructure. Compressive strength has also been experimentally determined for PBZT fibres coated with a thin layer of aluminium. The correlation between the theoretical and experimental data has been established. There is good potential for the improvement of compressive strength of rigid-rod polymeric fibres by coating them with a sufficiently thick shell of a rigid material; however, the maximum thickness of 83.3 nm used in this study is insufficient to effect any significant improvement in the compressive strength.

Several factors to be considered during the selection of a suitable coating material have been identified. Because most of the buckling strength of the coated fibre derives from that of the coating material, the stiffness of the latter should be sufficiently high. A high modulus of the coating material also gives a higher value for the modulus of the coated fibre. The specific modulus, which also takes into consideration the density of the coated fibre, can be used as a criterion to select the coating material, a value close to that of the original rigid-rod fibre being preferred. The coating material should also have a good adhesion characteristic with the polymer fibre in order to permit efficient transfer of the compressive load.

Finally, problems associated with coating the fibres have been identified. Extreme care must be exercised during the coating process in order not to damage the fibre prior to testing and adversely influencing the final properties. In order to incorporate a coupling agent between the fibrils, which may be one of the best means to improve fibre compressive strength [8], the material must be infiltrated while the fibre structure is still open and permeable; this is the case while the fibre is wet, immediately after spinning the fibre. Alternative detection methods may also need to be devised in order to identify more accurately defects in the fibre beneath the coating.

Acknowledgement

This research was supported by the US Air-Force Materials Laboratory under Contracts F33615-88-C-5420 and F49620-88-C-0053. In addition, the authors acknowledge the help of P. Zhang, Pennsylvania State University, in coating the PBZT fibres, and Gary Price, University of Dayton Research Institute, in obtaining scanning electron micrographs of the samples.

References

1. W. W. ADAMS and R. K. EBY, *MRS Bull.* **XII**(8) (1987) 22.
2. S. J. DETERESA, R. S. PORTER and R. J. FARRIS, *J. Mater. Sci.* **20** (1985) 1645.

3. D. C. MARTIN and E. L. THOMAS, *ibid.* **26** (1991) 5171.
4. H. H. CHUAH, T. T. TSAI, K. H. WEI, C. S. WANG and F. E. ARNOLD, in "ACS PMSE Proceedings" Vol. 60, edited by W. W. Adams and R. K. Eby (American Chemical Society, Washington, DC, 1989) p. 517.
5. C. Y-C. LEE and U. SANTHOSH, Air-Force Technical Report, WRDC-TR-90-4023 (1990).
6. T. D. DANG, L. S. TAN, K. H. WEI, H. H. CHUAH and F. E. ARNOLD, in "ACS PMSE Proceeedings", Vol. 60, edited by W. W. Adams and R. K. Eby (American Chemical Society, Washington, DC, 1989) p. 424.
7. R. F. KOVAR, R. HAGHIGHAT and R. W. LUSIGNEA, in "MRS Symposium Proceedings", Vol. 134 (Materials Research Society, Pittsburgh, PA, 1989) p. 389.
8. C. Y-C. LEE and U. SANTHOSH, *Polym. Eng. Sci.* (1991), *submitted.*
9. S. J. DETERESA, R. S. PORTER and R. J. FARRIS, *J. Mater. Sci.* **23** (1988) 1886.
10. K. E. NEWMAN, P. ZHANG, L. J. CUDDY and D. L. ALLARA, *J. Mater. Res.* **6**(7) (1991) 1580.
11. S. P. TIMOSHENKO and J. M. GERE, "Theory of Elastic Stability", 2nd Edn (McGraw-Hill, New York, 1961) Ch. 11.
12. P. SEIDE, *J. Aero. Sci.* **29** (1962) 851.
13. F. J. McGARRY and J. E. MOALLI, *Polymer* **32** (1991) 1811.
14. S. R. ALLEN, *J. Mater. Sci.* **22** (1987) 853.
15. K. E. NEWMAN, PhD thesis, Pennsylvania State University (1991).

Received 2 April 1993
and accepted 7 September 1994